HHS Public Access

Author manuscript

J Mater Chem B. Author manuscript; available in PMC 2019 August 21.

Published in final edited form as:

J Mater Chem B. 2018 August 21; 6(31): 5080–5090. doi:10.1039/C8TB00804C.

Cancer cell targeting, controlled drug release and intracellular fate of biomimetic membrane-encapsulated drug-loaded nano-graphene oxide nanohybrids

Kun Ma[#a,b,§,*], **Duo Fu**[#a,§], **Yajun Liu**[a], **Rui Dai**[a], **Dongli Yu**[a], **Zhaoming Guo**[a], **Changhao Cui**[a], **Li Wang**[a], **Jinaqiang Xu**[a], and **Chuanbin Mao**[b,c,*]

[a]School of Life Science and Medicine, Dalian University of Technology, Panjin 124221, China

[b]Department of Chemistry and Biochemistry, University of Oklahoma, OK 73019, USA

[c]School of Materials Science and Engineering, Zhejiang University, Hangzhou, Zhejiang 310027, China.

[#] These authors contributed equally to this work.

Abstract

Nano-graphene oxide (NGO) has been proposed as a novel drug carrier. However, the poor biocompatibility and physiological stability as well as lack of cancer targeting capability have limited its further applications in cancer therapy. To solve this problem, we developed a novel nanohybrid of NGO/DOX@SPC-FA by first allowing soy phosphatidylcholine membrane (SPC) to encapsulate DOX-loaded NGO (NGO/DOX) and then modifying the SPC membrane with PEGylated lipid-FA conjugate to achieve the display of cancer targeting FA on the nanohybrid surface. The SPC membrane (mimicking cell membrane) enabled the resultant nanohybrids (NGO/DOX@SPC-FA) to exhibit good stability and biocompatibility, high drug loading capability, efficient cellular uptake, and controlled drug release. Moreover, compared with NGO/DOX and SPC-modified NGO/DOX (NGO/DOX@SPC), the FA-modified NGO/DOX@SPC nanohybrids (NGO/DOX@SPC-FA) could deliver NGO/DOX to cancer cells with improved delivery and killing efficacy due to the presence of FA targeting motifs on the surface. The NGO/DOX@SPC-FA nanohybrids were found to be internalized specifically by FA-positive cancer cells (Hela cells) through both macropinocytosis-directed engulfment and clathrin-dependent endocytosis, and then become localized into the lysosomes. In vivo biodistribution study showed that NGO/DOX@SPC-FA had a high tumor targeting ability because of the active targeting mechanism with folate modification. In vivo antitumor therapy study demonstrated NGO/DOX@SPC-FA could significantly inhibit tumour growth and prolong the survival time of mice. Our results suggest that NGO/DOX@SPC-FA, as a novel drug delivery system with high drug loading and targeted delivery efficiency, holds promise for future cancer therapy.

[†]Electronic Supplementary Information (ESI) available: Fig. S1, XPS spectrum of NGO; Fig. S2, Representative photos of tumor tissues obtained in different groups after 14 days of treatment.

[*]Corresponding author: makunonline@163.com; cbmao@ou.edu.

Conflicts of interest

The authors declare no conflict of interest.

Graphical abstract

The FA-modified nanohybrids of NGO/DOX@SPC-FA could deliver DOX to cancer cells and tumor tissues with improved delivery and inhibition efficacy.

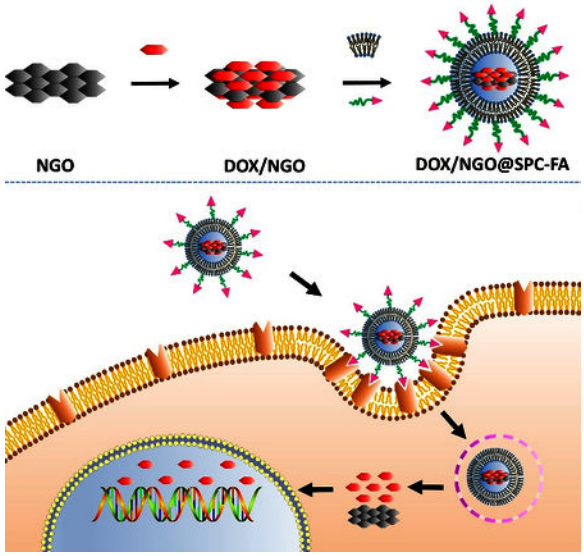

Introduction

Driven by the most updated development of materials chemistry[1, 2] and analytical sciences[3], nanoparticles-based drug delivery systems (DDSs) have been utilized in preclinical and clinical cancer therapy. They can improve therapeutic effects while decreasing side effects of anticancer drugs. Although the nanoscale DDSs such as hydrogels[4], micelles[5], and liposomes[6] nanoparticles have attracted attention for their performance in the delivery of many anticancer drugs, they have many limitations in low drug loading efficiency and poor physiological stability.

Owing to their large specific surface area[7, 8], large drug-loading capacity[9], and good passive tumor targeting[10], graphene and its derivatives have emerged as a promising nanocarrier for hydrophobic cancer therapeutics such as doxorubicin (DOX). This is because DOX and graphene (or its derivatives) could bind each other by both hydrophobic and π-π stacking interactions, promoting DOX loading on the graphene-based substrates. However, graphene-based substrates, such as nanoscale graphene oxide (NGO), are not stable in the aqueous solution after loaded with hydrophobic drugs, greatly restricting their application as a drug carrier. Therefore, it is still a challenge to develop a simple and efficient approach to functionalizing NGO for better physiological stability.

PEGylation of NGO is a frequently-used method to improve its hydrophilicity and biocompatibility[11]. However, PEGylation of NGO needs several chemical synthesis steps, resulting in low yield but high cost. In the past few years, many alternative methods were investigated to improve its physiological stability, but the final effect was far from satisfactory. Lipid bilayers exhibit physicochemical properties similar to cell membranes.

Thus, they were employed as a promising cloak for increasing the stability and biocompatibility of some inorganic nanoparticles. For example, liposomes derived from zwitterionic DOPC or cationic DOTAP, have been used to modify nanomaterials such as nanodiamond and carbon nanotubes[12, 13].

Inspired from such progress, in this study we first used zwitterionic soy phosphatidylcholine (SPC) liposomes as a biomimetic membrane to "wrap" hydrophobic NGO/DOX complex (DOX-loaded NGO) to form an NGO/DOX@SPC nanohybrids (Fig. 1). The lack of active cancer cell targeting and subsequently a poor cancer cell internalization will limit the therapeutic effect of NGO/DOX@SPC in drug delivery. To address this challenge, folic acid (FA) was introduced into NGO/DOX@SPC nanohybrids, and the DSPE lipid molecule of PEGylated FA-DSPE conjugate can be inserted into the lipid bilayer of NGO/DOX@SPC, leaving the FA motif protruding from the nanohybrids surface for cancer cell targeting. FA is a water-soluble B vitamin that is nonimmunogenic. It is capable of selectively binding to the folate receptor (FR) [14], a glycoprotein that is specifically recognized by FA [15]. Because FA has a high affinity to FR and the surface of a variety of human cancerous cells overexpress the FR, allowing FA to be presented on the surface of nanohybrids has been a successful strategy for enhancing the cancer targeting capability of the nanohybrids [16, 17]. Herein, we introduced FA to the surface of NGO/DOX@SPC to construct a novel active cancer-targeting DDS, NGO/DOX@SPC-FA. Our study showed NGO/DOX@SPC-FA exhibited excellent cancer cell targeting ability as well as outstanding stability in the physiological environment.

Experimental Section

Materials

Multilayer Graphene flake was obtained from Hengqiu Tech Inc. Potassium permanganate ($KMnO_4$, 99%), hydrochloric acid (HCl, 37%), sulfuric acid (H_2SO_4, 98%), hydrogen peroxide (H_2O_2, 30%), and anhydrous chloroform were obtained from Tianjin Damao Chemical Reagent Co. China. Doxorubicin hydrochloride (DOX) was purchased from Shanghai Yijing Industrial Co. SPC and the FA containing polyethylene glycol (PEG) distearoylphosphatidylethanolamine (DSPE-PEG_{2000}-Folate) were bought from Ponsure Biotechnology Co. 3-(4,5-dimethylthiazol-2-yl)-2,5-diphenyltetrazolium bromide (MTT), were purchased from Shanghai EKEAR Bio@Tech Co. LTD. LysoTracker-Red and Hoechst 33342 were obtained from Beyotime Biotechnology Co. Penicillin, streptomycin, RPMI 1640 culture medium, and fetal bovine serum (FBS) were obtained from Zhejiang Tianhang Biotechnology Co. Ltd. Double distilled water was obtained from Milli-Q system of Millipore Co., USA. Chlorpromazine (CPZ), methyl-β-cyclodextrin (MCD), and amiloride (AMI) were bought from Sangon Biotech (shanghai) Co., Ltd. Sodium dihydrogen phosphate, methanol and glacial acetic acid were purchased from Shanghai MACKLIN Chemical Reagent Co., LTD.

Preparation of NGO Nanosheet

NGO was produced using a modified Hummer's method[18, 19] with multilayered graphene as an original material. The highly oxidized NGO was cracked and exfoliated by the sonication

to obtain nano-sized and single layer NGO. The NGO was analyzed by UV-vis spectra, Attenuated Total Refraction-Fourier transform infrared spectroscopy (ATR-FTIR), Raman spectroscopy, and dynamic light scattering (DLS). We used X-ray photoelectron spectroscopy (XPS) characterization to confirm that the metal ions had been removed from NGO.

DOX Loading onto NGO to form NGO/DOX Complex

1 mg NGO was suspended in 5 mL of DOX solution (0.6 mg/mL). Then we used NaOH to adjust the pH value to improve the binding between DOX and NGO nanosheet[20, 21]. The suspension was stirred and centrifuged repeatedly to remove the unloaded DOX. The pellet after the centrifugation was dispersed in water. The amount of the loaded DOX could be determined by using the following equation on the basis of measured UV-Vis absorption at 490 nm.

Loading Content (LC%) = (Weight of loaded DOX) / (Weight of NGO)

Assembly of Lipid Bilayer Membrane on NGO/DOX Complex to form NGO/DOX@SPC-FA Nanohybrids

The biomimetic membrane was composed of soy phosphatidylcholine membrane (SPC) and Folate-(polyethylene glycol)-distearoylphosphatidylethanolamine (DSPE-PEG_{2000}-FA) with a mass ratio of 5: 1, namely about 20% DSPE-PEG_{2000}-FA of total lipid. Briefly, SPC (3.2 mg) and DSPE-PEG_{2000}-FA (0.64 mg) were mixed in chloroform (2.4 mL) in round-bottom flask, 800 μL NGO/DOX suspension (1 mg/mL) was placed into the resultant solution and then repeatedly mixed by ultrasound and vortex. The chloroform was removed by N_2 and then the lipid bilayer would wrap the NGO/DOX to form NGO/DOX@SPC-FA. The method of constructing NGO/DOX@SPC was same as the above procedure except the absence of DSPE-PEG_{2000}-FA. The obtained NGO/DOX@SPC-FA was kept at 4° and used within one week.

Characterization of NGO/DOX@SPC-FA Nanohybrids

The morphologies of NGO/DOX@SPC-FA nanohybrids were verified by a Transmission electronic microscope (TEM). For TEM observation, the samples were dropped onto a copper grid. Then the samples were stained using phosphotungstic acid (1%, W:V). The samples were observed by TEM after air-drying. The size distribution and zeta potential were detected by DLS. The NGO/DOX@SPC-FA was also analyzed by ATR-FTIR, fluorescence spectrum, UV–vis spectrum and Raman spectroscopy.

pH Dependent Drug Release

For studying the in vitro DOX release, NGO/DOX@SPC-FA was dispersed in PBS with a varying pH value (7.4, 6.5, 5.3). Then, the dispersion was shaken at 100 rpm at 37° to imitate the body temperature in the dark condition. At the desired time intervals, 5 μL of the medium was taken out to determine the released DOX by using UV-Vis spectroscopy to measure the absorption at 490 nm. Then the 5 μL of fresh medium was added to the original medium to supplement the removed the media.

In vitro Cytotoxicity

MTT assay was used to characterize the cytotoxicity of each formulation (DOX, NGO, NGO/DOX, NGO/DOX@SPC, NGO/DOX@SPC-FA) on cancer cells (Hela) and non-cancer cells (293T) following our published protocol[22].

Cells Targeting Competitive Targeting Inhibition

Hela or 293T cells with a seeding density of 1×10^5 cells/well were cultured for one day. Then the cells were incubated first with FA (5 mg/mL) for 2 h, and with NGO/DOX@SPC-FA (10 μg/mL) for additional 2 h. The cells were then washed with PBS, collected with trypsin and lysed under ultrasonication using the RIPA Lysis Buffer. Then DOX was further extracted using 1% HCl. Finally, the fluorescence intensity of DOX in the supernatant was determined at the excitation/emission wavelength of 480/595 nm.

Cellular Uptake

After Hela or 293T cells (1×10^5 cells/well) were cultured for one day, nanohybrids, NGO/DOX@SPC-FA or NGO/DOX@SPC (10 μg/mL DOX), were placed into the medium and incubated for one day, with free DOX (10 μg/mL) as a control group. Then, the amount of DOX in the supernatant was determined by a fluorescence detector.

Endocytosis Pathways

After Hela or 293T cells were cultured for 24 h at 37°, the media was removed. Then the cells were pre-incubated with different specific endocytosis inhibitors for half an hour. Subsequently, the cells were treated with NGO/DOX@SPC-FA (10 μg/ml) in the presence of inhibitors (CPZ, MCD, or AMI) at 37 °C for another 24 h. Then the cellular uptake of the nanohybrids was quantified as above.

Lysosomes Co-localization

The intracellular delivery of NGO@SPC-FA nanohybrids were investigated by using Coumarin-6 labeled NGO@SPC-FA (NGO@SPC/Cou6-FA). Briefly, Hela cells were incubated with NGO@SPC/Cou6-FA for 1 h, followed by washing with PBS. Then 100 nM of Lyso-Tracker Red was added to stain lysosomes for 30 min. The staining agent was removed by washing the cells. Then the cells were treated with 4% paraformaldehyde for 20 min to achieve fixing. Finally, Hoechest 33342 was used to stain the nuclei for another 20 min. The stained cells were visualized under confocal laser scanning microscopy (CLSM).

Intracellular Localization

The double-labeling of NGO/DOX@SPC/Cou6-FA was carried out by mixing Cou6 (0.001wt% in the total lipids), which served as a fluorescent probe to label the phospholipid bilayer, and DOX, which acted as another fluorescent probe. The localization of SPC and NGO/DOX was visualized to investigate the subcellular distribution of the nanohybrids in Hela cells. The cells were incubated on the cover slide for 24 h at 37° and incubated with NGO/DOX@ SPC/Cou6-FA (with a concentration of Cou6 and DOX of 320 ng/ml and 200 μg/ml) for 1 h. After incubation, Hoechest 33342 was used to stain nuclei. The cells were washed and observed under CLSM.

In vivo target distribution and antitumor therapy

All animal experiments were approved by the Institutional Animal Care and Use Committee of Dalian University of Technology. The four to five weeks old female nude mice were used for tumor transplantation. The cervical cancer Hela cells (1×10^7cells/mouse) were subcutaneously inoculated in the flank of nude mice with for the construction of the tumor xenograft model.

In the biodistribution study, the tumor bearing nude mice were sacrificed at 5 h and 24 h after intravenous injection of free DOX (5mg/kg), NGO/DOX@SPC or NGO/DOX@SPC-FA (5 mg equivalent DOX per kg animal for NPs). The major tissues (0.05 g of each) were weighed and homogenized in 0.2 mL of lysis buffer (Beyotime, China) for 20 min. For DOX extraction, the tissue lysate was mixed with 0.2 mL methanol. After strong vortexing and homogenization for another 20 min, the whole mixture was centrifuged at 13000 rpm for 10 min, the fluorescence of the supernatant was measured by high-performance liquid chromatography (HPLC) analysis. A mixture of sodium dihydrogen phosphate (50 mM, pH 7.0) and methanol (40:60, v/v) containing 20 mM glacial acetic acid was used as a mobile phase. The flow-rate of the mobile phase was set at 1 mL/min.

In the in vivo antitumor therapy study, when the tumor reached ~100 mm^3 in volume, the mice were randomly divided into four different treatment groups: (i) Saline; (ii) free Dox (5mg/kg); (iii) NGO/DOX@SPC and (iv) NGO/DOX@SPC-FA. The dose for the last two groups is 5 mg equivalent DOX per kg animal. The tumor volumes were measured every 2 days for 14 days and then calculated with volume = $1/2\ (LW)^2$, where L was the maximum diameter and W was the minimum diameter of a tumor. Body weights and survival curves were also recorded after the treatments.

Statistical Analysis

The experimental data were expressed in the form of mean ± standard deviation. Two-tailed Student's t -test or one-way ANOVA was used to test the statistical difference between groups with a statistical significance level of $P < 0.05$ and an extreme significance level of $P < 0.01$.

Results and Discussion

The hydrophobic property of the NGO/DOX complex was enhanced after DOX was adsorbed onto the NGO through **π-π** stacking[23], due to the partial reduction of NGO and the expansion of the hydrophobic region[24] during drug loading process. Moreover, the hydrophobic property of the NGO/DOX caused the zwitterionic liposomes to be adsorbed on the hydrophobic regions to become ruptured[25, 26]. Nevertheless, at the edge of NGO, some oxygen-bearing groups such as carboxyl groups were still present, which provided sites for electrostatic attraction of the phospholipid head of zwitterionic liposomes[27], promoting the encapsulation of NGO/DOX complex by the liposomes. Our design and construction strategy of NGO/DOX@SPC-FA was illustrated in Fig. 1. Firstly, NGO was prepared according to the reported method[18, 19]. Then, DOX was loaded onto the NGO through **π-π** stacking and hydrophobic interaction to form NGO/DOX complex. Finally, NGO/DOX was

co-coated with SPC and DSPE-PEG_{2000}-FA by means of hydrogen-bonding interaction[28]. It was expected that this biomimetic membrane-modified DOX/NGO could improve the long-term blood circulation and enter tumor tissue by means of EPR effects. After the FA bound the folate receptor on the cancer cells, the nanohybrids were endocytosed, enhancing the cancer targeting capability of the nanohybrids significantly. Once the nanohybrids were uptaken, DOX was released quickly from the nanohybrids in acidic lysosomes due to the protonation effect. Then, the released DOX entered cell nucleus to take its effect of killing the cancer cells.

Characterization of NGO/DOX@SPC-FA nanohybrid

NGO was obtained by a modified Hummers' method[18, 19]. As revealed in Fig.2, after the oxidation of graphene sheet, the NGO was obtained. The multilayered graphene had a sharp and strong absorption peak at 1576 cm^{-1}. The G peak of the graphene oxide became wider and shifted to 1585 cm^{-1}, and the D peak at 1345 cm^{-1} becomes stronger after oxidation. UV-vis spectrum showed that by using the modified Hummer's method, the characteristic absorption peaks of C=O and C=C at 230 nm and 300 nm appeared. FT-IR spectrum showed that C=O groups with a band at 1730 cm^{-1} were present at the edge of the NGO structure layer. TEM imaging showed the NGO nanosheet was nearly 40 nm wide (Fig. 2D). The absence of the Mn 2p peak for NGO after dialysis suggested the successful purification of NGO (Fig. S1).

Fig. 3A showed that the morphology of NGO/DOX@SPC-FA was round with a size of 123.0 nm. The nanoparticle size increased with the co-assembly of SPC and DSPE-PEG_{2000}-FA on the surface of NGO/DOX complex. Zeta potential (ZP) is important for the stability of nanoparticles in various physiological solutions (such as PBS, 1640 medium, and complete medium) and their interaction with cell membrane[29]. As displayed in Fig. 3B, the surface charge of NGO was −54 mV, which could be attributed to the carboxyl group, carbonyl group and hydroxyl group on the surface of the NGO nanosheets. After NGO was loaded with DOX, the ZP of the NGO/DOX complex was increased to −30 mV, because the positively charged amino groups on the DOX were neutralized by the partial negative charge of the NGO. The NGO/DOX@SPC exhibited a lower ZP value at −57 mV after the NGO/DOX surface was coated with SPC. This change in ZP may be ascribed to that the amino group of DOX was shielded by the phospholipid bilayer, which indirectly confirmed that the phospholipid bilayer could be assembled on the NGO/DOX complex to form the integrated nanohybrids. After the NGO/DOX@SPC was functionalized with DSPE-PEG_{2000}-FA, the ZP of the resultant NGO/DOX@SPC-FA was still negative but increased from −55 mV to −44 mV. This result could be due to the presence of the amino group in the FA exposed on the nanohybrids. This also indicated that DSPE-PEG_{2000}-FA was embedded into the lipid bilayer of SPC membrane while leaving the FA protruding from the surface for cancer cell targeting.

In Fig. 3C, we used the ZP value to evaluate the stability of NGO/DOX@SPC-FA nanohybrids in the physiological solution. Although the ZP of the nanohybrids varied in the different physiological solutions (PBS, 1640 medium, 1640 medium with 10%FBS), the nanohybrids were stable under the various physiological conditions even after 10 days.

Usually, DOX causes the stacking and aggregation of large GO sheets, but DOX-induced aggregation was significantly reduced with nano-GO, and the presence of lipid bilayers from the liposomes could further minimize it [13]. It was concluded that the dispersion of NGO could further be improved by phospholipid bilayers adsorption and NGO/DOX@SPC-FA nanohybrids are thus suitable for future clinical application because of their long-term stability.

The surface characterization of the nanohybrids was further evaluated using FT-IR spectroscopy (Fig. 4A and B). The peak for C=O of NGO (at 1732 cm^{-1}) and the peak for C=O of DOX (1730 cm^{-1}) were slightly shifted to 1717 cm^{-1} after the formation of the NGO/DOX complex (Fig. 4A), which confirmed that DOX was loaded onto the GO[30, 31]. After the NGO/DOX complex was encapsulated by SPC, the peaks appearing at 2852 and 2922 cm^{-1} could be assigned to νs(C-H) and νas(C-H) of $–CH_2$ in SPC (Fig. 4B,), respectively. This verified the presence of SPC in the nanohybrids. As for NGO/DOX@SPC-FA, the peak at 1628 cm^{-1} corresponding to -C=O- of amide in the DSPE-PEG_{2000}-FA indicated the existence of the targeting ligand FA on the nanohybrids.

Furthermore, UV-vis spectroscopy was performed to confirm the formation of nanohybrids (Fig. 4C and D). NGO showed its signature absorption peak at 232 nm, and DOX presented strong absorption at 233, 253, 291 and 480 nm (Fig. 4C). The loading of DOX on the NGO resulted in the shift of the peaks of DOX from 233 and 480 nm to 235 and 490 nm, respectively. This suggests the donor-acceptor interactions between DOX and NGO[32, 33]. The characteristic peaks of FA at 280 and 475 nm were also observed in Fig. 4D. These observations confirmed the integration of DSPE-PEG_{2000}-FA into NGO/DOX@SPC nanohybrids.

π-π stacking is the most important interaction between the NGO and DOX. It was reported that a photo induced electron-transfer process or efficient energy transfer could occur along NGO/DOX complex interface[34, 35]. Therefore, NGO/DOX complex exhibited significant quenching of the fluorescence of the DOX at the same excitation wavelength. When SPC was coated onto the NGO/DOX complex, the quenching effect was also observed as shown in Fig. 5, which indicated that the phospholipid bilayers did not compete with DOX to bind NGO and did not adsorb DOX from NGO. Furthermore, after SPC and DSPE-PEG_{2000}-FA were co-coated on the NGO/DOX complex, the same result was found. These results implied that the DOX wasn't exfoliated from NGO while being protected by the lipid bilayers, making it possible to achieve the pH-sensitivity and sustained release property of the nanohybrids as a carrier [13].

pH Dependent Drug Release

To confirm the sustained release and pH sensitive properties of the nanohybrids, the drug release of NGO/DOX@SPC-FA in vitro was investigated. When the pH was set at 7.4, 40% of the DOX was released from the nanohybrids in two days (Fig. 6), suggesting that the biomimetic membrane can prevent the drug burst-release from the NGO/DOX@SPC-FA nanohybrids in the normal tissues. In contrast, DOX release level of 90% and 85% was found at pH 5.3 and pH 6.5 during 48 h, respectively, which implied that the amino protonation in the DOX led to hydrophilic enhancement and the consequent improvement of

the drug release from the nanohybrids. The pH responsive drug release of NGO/DOX@SPC-FA would be of great benefit to controlled drug release at the acidic tumor environment and lysosomes, improving targeted drug delivery to tumors and decreasing undesirable side effects.

MTT Assay

The cytotoxicity of NGO, NGO@SPC, NGO@SPC-FA without DOX was evaluated by MTT assay in 293T cells and Hela cells. No obvious toxicity at all formulation concentrations of these carriers was observed (Figure 7). These results suggest that these nanoparticles are biocompatible, and the phospholipid bilayers did not inhibit the NGO uptake by the cells.

The toxicity of the DOX, NGO, NGO/DOX and NGO/DOX@SPC-FA was studied by using MTT assay (Fig.8). The free DOX showed significant cytotoxicity at 5 μg/mL, and no more than 20% of the cells could survive at that concentration. However, after the DOX was loaded on the NGO, the cytotoxicity of the NGO/DOX complex was reduced. The NGO loaded with the DOX could not exert its pharmacological effects. Only if the DOX was dissociated from NGO, would the DOX kill the cancer cells. The cytotoxicity of the NGO was relatively negligible. The NGO/DOX@SPC-FA showed lower cytotoxicity than the free DOX at 5 μg/mL. But its cytotoxicity was significantly increased in comparison to NGO/DOX and free DOX at higher concentrations. This indicated that the nanoparticles exhibited the ability to kill cancer cells more effectively after modification by the targeting FA. It is known that the free zwitterionic liposomes were hard to be internalized by the cells. However, in this study, the NGO/DOX@SPC-FA nanohybrids were highly stable and could be uptaken by the cells efficiently. Hence, we believed that the phospholipid bilayers on the nanohybrids could facilitate the cellular uptake of NGO/DOX complex. After loaded with the DOX, the nanohybrids could effectively kill cancer cells, even more efficiently than the free DOX at the concentrations above 10 μg/mL. Moreover, FA on the surface of the nanohybrids could more easily bind with folate receptor of cancer cells to facilitate the endocytosis of the nanohybrids and kill the cancer cells.

Competitive Targeting Inhibition

Selective accumulation of the nanohybrids in cancer cells is of great concern for targeted cancer therapy. In order to show that the increased cellular uptake of NGO/DOX@SPC-FA nanohybrids was attributed to the ligand-receptor interaction but not to the non-specific adhesion, competitive targeting inhibition was performed in the Hela and 293T cells. Unlike 293T cells, Hela cells overexpress FA receptors. Before the nanohybrids were added for cell uptake investigation, the cells were pretreated with free FA for 30 min. As showed in Fig. 9, no obvious difference was observed in the uptake of the nanohybrids by the 293T cells between the cells pretreated with and without free FA. On the contrary, the pretreatment with FA significantly decreased the uptake of NGO/DOX@SPC-FA nanohybrids by Hela cells, suggesting that the FA pretreatment caused the FA receptors to be blocked and thus reduced the possibility for the FA-bearing nanohybrids to recognize the FA receptors. Thus, it can be concluded that the uptake of the NGO/DOX@SPC nanohybrids in cancer cells could be promoted by FA modification.

Cellular Uptake

Hela cells were used here to investigate whether FA-modified nanohybrids could increase the drug delivery to FA-overexpressing tumor cells. 293T cells were chosen, as a control cell with negative FA receptor expression. The DOX, loaded on NGO via π-π stacking, could serve as a red fluorescence probe to indicate the cellular uptake behavior of the nanohybrids. Specifically, two formulations (NGO/DOX@SPC, NGO/DOX@SPC-FA) with the same concentration of DOX were allowed to interact with Hela or 293T cells for 24 h. As shown in Fig. 10, compared with NGO/DOX@SPC, the cellular uptake of NGO/DOX@SPC-FA was increased significantly by two folds in Hela cells. Namely, after modification with DSPE-PEG_{2000}-FA, the drug delivery efficiency of the nanohybrids was nearly 2 times that of the unmodified ones. However, the intracellular content of the DOX in the 293T cells did not show significant difference for the two formulations with and without FA modification. This result indicated that the FA modification could facilitate the specifically targeted delivery of nanohybrids to FA-overexpressing tumor cells. Our result is consistent with the previous reports that ligand modified nanoparticles could enhance the cellular uptake via receptor-mediated endocytosis[36, 37].

Endocytosis Pathways

A detailed understanding of how nanoparticles getting into the cells were important to figure out the improved selectivity and less cytotoxicity of this new nanohybrid (NGO/DOX@SPC-FA). The endocytic pathways of NGO/DOX@SPC-FA were proved using various endocytosis inhibitors such as methyl-β-cyclodextrin (M-β-CD), chlorpromazine (CPZ), and amiloride (AMI). It is well known that CPZ (30 μg/ml) is the clathrin-mediated endocytosis inhibitor, AMI (150 μg/ml) is the macropinocytosis inhibitor, and M-β-CD (30 μg/ml) is the lipid raft inhibitor[38, 39]. As shown in Fig. 11, CPZ resulted in the decrease of 80% DOX uptake, suggesting that NGO/DOX@SPC-FA was predominantly endocytosed by a clathrin-mediated endocytic pathway. In addition, AMI also caused a mild reduction in the cellular DOX uptake, implying that macropinocytosis restrained the endocytic cellular uptake. The decreased cellular uptake of the nanohybrids in the presence of CPZ and AMI was consistent with the results of most polymer-based [40–42] and GO-based [43] nanoparticles. Of the three endocytosis inhibitors applied, only M-β-CD played no obvious effect on the uptake of the nanohybrids, suggesting that the lipid raft might not participate in the uptake of NGO/DOX@SPC-FA nanohybrids.

Lysosomes Co-localization

We then used confocal microscopy to confirm the intracellular distribution after the endocytosis of the nanohybrids. The phospholipid bilayers of NGO@SPC-FA were labeled with Coumarin-6 (NGO@SPC/Cou6-FA) and lysosomes were labeled with Lyso-tracker Red. As shown in Fig. 12, after the treatment of the NGO@SPC/Cou6-FA for 1 h, most of the endocytosed NGO@SPC/Cou6-FA nanohybrids were positioned in lysosomes labeled with red fluorescence. The overlap yellow fluorescence (Fig. 12D) confirms that after 1 h of incubation, NGO@SPC/Cou6-FA was endocytosed by Hela cells through both macropinocytosis-mediated engulfment and clathrin-dependent endocytosis (Fig.11) and then be localized into the lysosomes[44].

Intracellular Localization

Intracellular co-location of the SPC and NGO/DOX parts of the nanohybrids were investigated by CLSM with the specific fluorescent probes, including Cou6 (for labeling the phospholipid bilayers) and the auto-fluorescent DOX (for labeling NGO and thus showing the intracellular distribution of NGO). The overlap yellow fluorescence as shown in Fig. 13 revealed that SPC and NGO/DOX of NGO/DOX@SPC-FA stayed together after the nanohybrids were taken up through the endocytosis by Hela cells. Namely, the nanohybrids were not dissociated before and after entering the tumor cells due to the special micro-environment of tumor.

In vivo biodistribution and antitumor therapy

To evaluate the tumor-targeting ability and antitumor capacity of the nanohybrids in vivo, cervical tumor-bearing mouse model was established by subcutaneous injection of Hela cells in the flank of femina nude mice. The in vivo biodistribution of nanohybrids was investigated after intravenous administration into the cervical tumor-bearing mice by quantitatively detecting the DOX content in different tissues, including heart, liver, spleen, lung, kidney and tumor. The tumor-bearing mice were sacrificed at 5 h and 24 h after the injection of NGO/DOX@SPC and NGO/DOX@SPC-FA, and the major organs were harvested and homogenized for DOX extraction [45]. Then, the concentration of DOX in each organ was measured by HLPC. Free DOX was used as a control.

At 5 h post-injection, the DOX distribution in all tissues in the free DOX group was higher than that in other groups (NGO/DOX@SPC and NGO/DOX@SPC-FA). Such difference is more significant in heart, suggesting that the cardiotoxicity of the first group was more significant than the latter two (Fig. 14A). The DOX distributions in the tumor tissues among all groups were relatively negligible. However, the concentration of DOX in all tissues in the free DOX group after 24 h dropped significantly (Fig. 14B), indicating the rapid clearance of the free DOX from body. But the DOX concentration in the groups of NGO/DOX@SPC and NGO/DOX@SPC-FA was decreased slightly, suggesting that these two groups could stay in vivo for a longer time to take effects. Notably, the DOX biodistribution in tumor at 24 h was increased when compared to that at 5 h for the groups of NGO/DOX@SPC and NGO/DOX@SPC-FA. Furthermore, the DOX uptake of NGO/DOX@SPC-FA in the tumor was much higher than that of the undecorated NGO/DOX@SPC and even three fold higher than that of free DOX (Fig. 14), suggesting that the NGO/DOX@SPC-FA nanohybrid was able to provide high concentration of DOX in the tumor after the prolonged systemic circulation for improved therapeutic effect[46]. It was demonstrated that NGO/DOX@SPC-FA had a high tumor targeting ability as a result of the active targeting mechanism with folate modification.

To study the therapeutic efficacy of NGO/DOX@SPC-FA nanohybrid for tumor therapy, the mice were intravenously injected with saline, free DOX, NGO/DOX@SPC, or NGO/DOX@SPC-FA (Fig. 15). In the following 14 days, the tumor volumes and body weights of the mice were closely measured. As shown in Figure 15 A, the tumor grew quickly in the following days in the saline group, indicating that free DOX was ineffective in tumor suppression, likely due to the limited tumor accumulation of the DOX. Compared to the free DOX group, the NGO/DOX@SPC group showed better tumor growth delay with an

inhibition rate of 58.3%. Notably, after the mice were treated with NGO/DOX@SPC-FA, they presented the most significant inhibition of tumor growth with an inhibition rate of 75.1%. The representative photos of tumor tissues obtained in different groups were showed in Fig. S2.

Intriguingly, according to the profile of the percent survival rate, a prolonged median survival time was observed in mice treated with nanohybrids (26 days for NGO/DOX@SPC, 36 days for NGO/DOX@SPC-FA), which was about 2 times longer than that for the mice treated with saline and free DOX (14 days for saline, 20 days for free DOX) (Fig. 15 D). Interestingly, 40% mice treated with NGO/DOX@SPC-FA survived for over 40 days.

Conclusions

In this study, we developed a novel therapeutic agent by using soy phosphatidylcholine membrane (SPC) to encapsulate the DOX-loaded NGO to enhance its biocompatibility and biostability. The resultant nanohybrid NGO/DOX@SPC was further modified with FA for targeting cancer cells, leading to the formation of NGO/DOX@SPC-FA nanohybrids with good biocompatibility, outstanding drug loading capability, efficient cellular uptake, and excellent controlled sustained release. Moreover, the NGO/DOX@SPC-FA was strongly sensitive to the pH value and could release the drug in a sustained manner at the acidic conditions unique for the tumor environment. Importantly, the in vitro cellular uptake and cell targeting assays demonstrated that NGO/DOX@SPC-FA could target specifically Hela cells in contrast to NGO/DOX@SPC. The nanohybrids were found to be internalized specifically by Hela cells though both macropinocytosis-directed engulfment and clathrin-dependent endocytosis, and then be localized into the lysosomes. In vivo experiments demonstrated that the NGO/DOX@SPC-FA nanohybrid was able to target tumor and showed better tumor therapeutic effect. Overall, this work demonstrated a novel cancer-targeting drug carrier with good solubility and stability, biocompatibility and target-specificity.

Supplementary Material

Refer to Web version on PubMed Central for supplementary material.

Acknowledgements

This study was supported by the Scientific Research Foundation for the Returned Overseas Chinese Scholars from the Ministry of Education, National Natural Science Foundation of China (51673168, 31670767, 81603049), Liaoning Provincial Natural Science Foundation of China (20170540155). KM and CBM would also like to thank the financial support from National Institutes of Health (CA200504, CA195607, and EB021339).

Notes and references

1. Li HG, Xie C, Lan RF, Zha S, Chan CF, Wong WY, Ho KL, Chan BD, Luo YX, Zhang JX, Law GL, Tai WCS, Bunzli JCG and Wong KL, J Med Chem, 2017, 60, 8923–8932. [PubMed: 28991460]
2. Li H, Harriss BI, Phinikaridou A, Lacerda S, Ramniceanu G, Doan B-T, Ho K-L, Chan C-F, Lo W-S, Botnar RM, Lan R, Richard C, Law G-L, Long NJ and Wong K-L, Nanotheranostics, 2017, 1, 186–195. [PubMed: 29071187]

3. Li H, Lan R, Chan CF, Jiang L, Dai L, Kwong DW, Lam MH and Wong KL, Chem Commun (Camb), 2015, 51, 14022–14025. [PubMed: 26257074]
4. Wang H, Luo Z, Wang Y, He T, Yang C, Ren C, Ma L, Gong C, Li X and Yang Z, Adv Funct Mater, 2016, 26, 1822–1829.
5. Huang F, Wang J, Qu A, Shen L, Liu J, Liu J, Zhang Z, An Y and Shi L, Angew Chem Int Ed Engl, 2014, 53, 8985–8990. [PubMed: 24985739]
6. Hofheinz RD, Gnad-Vogt SU, Beyer U and Hochhaus A, Anticancer Drugs, 2005, 16, 691–707. [PubMed: 16027517]
7. Dreyer DR, Park S, Bielawski CW and Ruoff RS, Chem Soc Rev, 2010, 39, 228–240. [PubMed: 20023850]
8. Liu Z, Robinson JT, Sun X and Dai H, J Am Chem Soc, 2008, 130, 10876–10877. [PubMed: 18661992]
9. Miao W, Shim G, Kang CM, Lee S, Choe YS, Choi HG and Oh YK, Biomaterials, 2013, 34, 9638–9647. [PubMed: 24016852]
10. Zhou T, Zhou X and Xing D, Biomaterials, 2014, 35, 4185–4194. [PubMed: 24513318]
11. Tan X, Feng L, Zhang J, Yang K, Zhang S, Liu Z and Peng R, ACS Appl Mater Interfaces, 2013, 5, 1370–1377. [PubMed: 23360681]
12. Ip AC, Liu B, Huang PJ and Liu J, Small, 2013, 9, 1030–1035. [PubMed: 23239613]
13. Wang F, Liu B, Ip AC and Liu J, Adv Mater, 2013, 25, 4087–4092. [PubMed: 23722422]
14. Salmaso S, Semenzato A, Caliceti P, Hoebeke J, Sonvico F, Dubernet C and Couvreur P, Bioconjug Chem, 2004, 15, 997–1004. [PubMed: 15366952]
15. Porta F, Lamers GE, Morrhayim J, Chatzopoulou A, Schaaf M, den Dulk H, Backendorf C, Zink JI and Kros A, Adv Healthc Mater, 2013, 2, 281–286. [PubMed: 23184490]
16. Zhu Y, Ikoma T, Hanagata N and Kaskel S, Small, 2010, 6, 471–478. [PubMed: 19943250]
17. Leamon CP and Reddy JA, Adv Drug Deliv Rev, 2004, 56, 1127–1141. [PubMed: 15094211]
18. Feng L, Yang X, Shi X, Tan X, Peng R, Wang J and Liu Z, Small, 2013, 9, 1989–1997. [PubMed: 23292791]
19. Feng L, Zhang S and Liu Z, Nanoscale, 2011, 3, 1252–1257. [PubMed: 21270989]
20. Liu Z, Sun X, Nakayama-Ratchford N and Dai H, ACS Nano, 2007, 1, 50–56. [PubMed: 19203129]
21. Liu Z, Fan AC, Rakhra K, Sherlock S, Goodwin A, Chen X, Yang Q, Felsher DW and Dai H, Angew Chem Int Ed, 2009, 48, 7668–7672.
22. Ma K, Wang DD, Lin Y, Wang J, Petrenko V and Mao C, Adv Funct Mater, 2013, 23, 1172–1181. [PubMed: 23885226]
23. Sun X, Liu Z, Welsher K, Robinson JT, Goodwin A, Zaric S and Dai H, Nano Research, 2008, 1, 203–212. [PubMed: 20216934]
24. Ma N, Zhang B, Liu J, Zhang P, Li Z and Luan Y, Int J Pharm, 2015, 496, 984–992. [PubMed: 26541300]
25. Ip ACF, Liu B, Huang P-JJ and Liu J, Small, 2013, 9, 1030–1035. [PubMed: 23239613]
26. Kong X, Lu D, Wu J and Liu Z, Langmuir, 2016, 32, 3785–3793. [PubMed: 27019394]
27. Li S, Stein AJ, Kruger A and Leblanc RM, J Phys Chem C, 2013, 117, 16150–16158.
28. Ma K, Fu D, Yu D, Cui C, Wang L, Guo Z and Mao C, Biomaterials, 2017, 121, 55–63. [PubMed: 28081459]
29. Tu Z, Wycisk V, Cheng C, Chen W, Adeli M and Haag R, Nanoscale, 2017, 9, 18931–18939. [PubMed: 29177354]
30. Yang X, Zhang X, Liu Z, Ma Y, Huang Y and Chen Y, J Phys Chem C, 2008, 112, 17554–17558.
31. Yang X, Lu Y, Ma Y, Li Y, Du F and Chen Y, Chem Phys Lett, 2006, 420, 416–420.
32. Yoshio M, Wang H and Fukuda K, Angew Chem Int Ed, 2003, 42, 4203–4206.
33. Nelson DJ and Brammer CN, Anal Bioanal Chem, 2010, 396, 1079–1086. [PubMed: 19760405]
34. Guo Z, Du F, Ren D, Chen Y, Zheng J, Liu Z and Tian J, J Mater Chem, 2006, 16, 3021–3030.
35. Baskaran D, Mays JW, Zhang XP and Bratcher MS, J Am Chem Soc, 2005, 127, 6916–6917. [PubMed: 15884911]

36. Yang K, Luo H, Zeng M, Jiang Y, Li J and Fu X, ACS Appl Mater Interfaces, 2015, 7, 17399–17407. [PubMed: 26196506]
37. Cheng W, Nie J, Xu L, Liang C, Peng Y, Liu G, Wang T, Mei L, Huang L and Zeng X, ACS Appl Mater Inter, 2017, 9, 18462–18473.
38. Sahay G, Alakhova DY and Kabanov AV, J Controlled Release, 2010, 145, 182–195.
39. Yan M, Du J, Gu Z, Liang M, Hu Y, Zhang W, Priceman S, Wu L, Zhou ZH, Liu Z, Segura T, Tang Y and Lu Y, Nat Nano, 2010, 5, 48–53.
40. Poon GMK and Gariépy J, Biochem Soc Trans, 2007, 35, 788–793. [PubMed: 17635149]
41. Futami J, Kitazoe M, Maeda T, Nukui E, Sakaguchi M, Kosaka J, Miyazaki M, Kosaka M, Tada H, Seno M, Sasaki J, Huh N-H, Namba M and Yamada H, J Biosci Bioeng, 2005, 99, 95–103. [PubMed: 16233763]
42. Fischer R, Köhler K, Fotin-Mleczek M and Brock R, J Biol Chem, 2004, 279, 12625–12635. [PubMed: 14707144]
43. Huang J, Zong C, Shen H, Liu M, Chen B, Ren B and Zhang Z, Small, 2012, 8, 2577–2584. [PubMed: 22641430]
44. Mo R, Sun Q, Li N and Zhang C, Biomaterials, 2013, 34, 2773–2786. [PubMed: 23352118]
45. Laginha KM, Verwoert S, Charrois GJ and Allen TM, Clin Cancer Res, 2005, 11, 6944–6949. [PubMed: 16203786]
46. Pakunlu RI, Wang Y, Saad M, Khandare JJ, Starovoytov V and Minko T, J Control Release, 2006, 114, 153–162. [PubMed: 16889867]

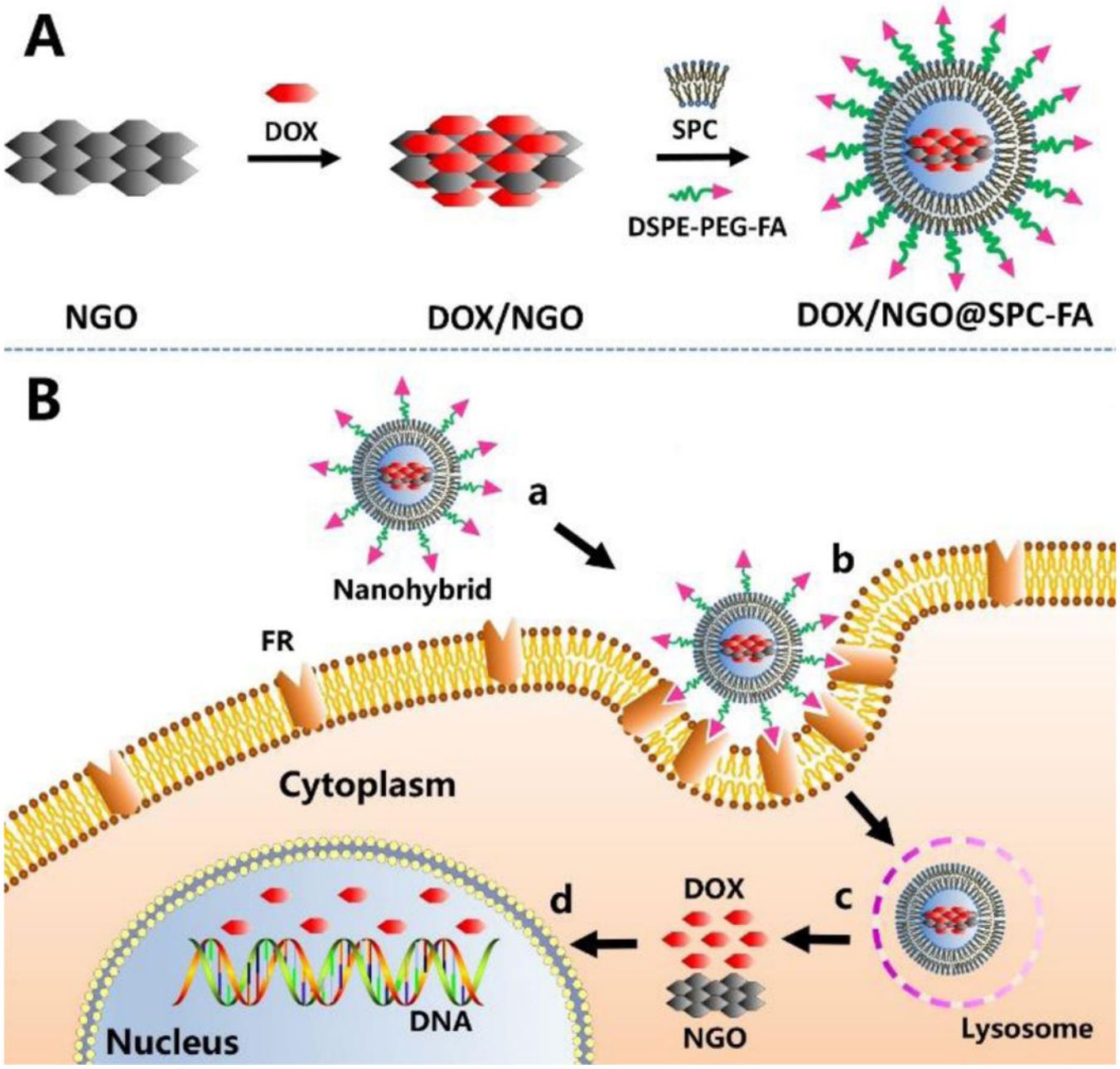

Fig. 1.

Schematic illustration of design and construction strategy of NGO/DOX@SPC-FA (A) and its targeting delivery process (B). The biomimetic membrane-modified nanohybrid could improve the long-term blood circulation and enter into tumor tissue by means of EPR effects (a). After FA bound with FR on cancer cells, the nanohybrid was endocytosed and entered into cells (b). In the cells, DOX released quickly from NGO in the low pH environment of lysosome (c). Then, DOX entered into cell nucleus to take its effect (d).

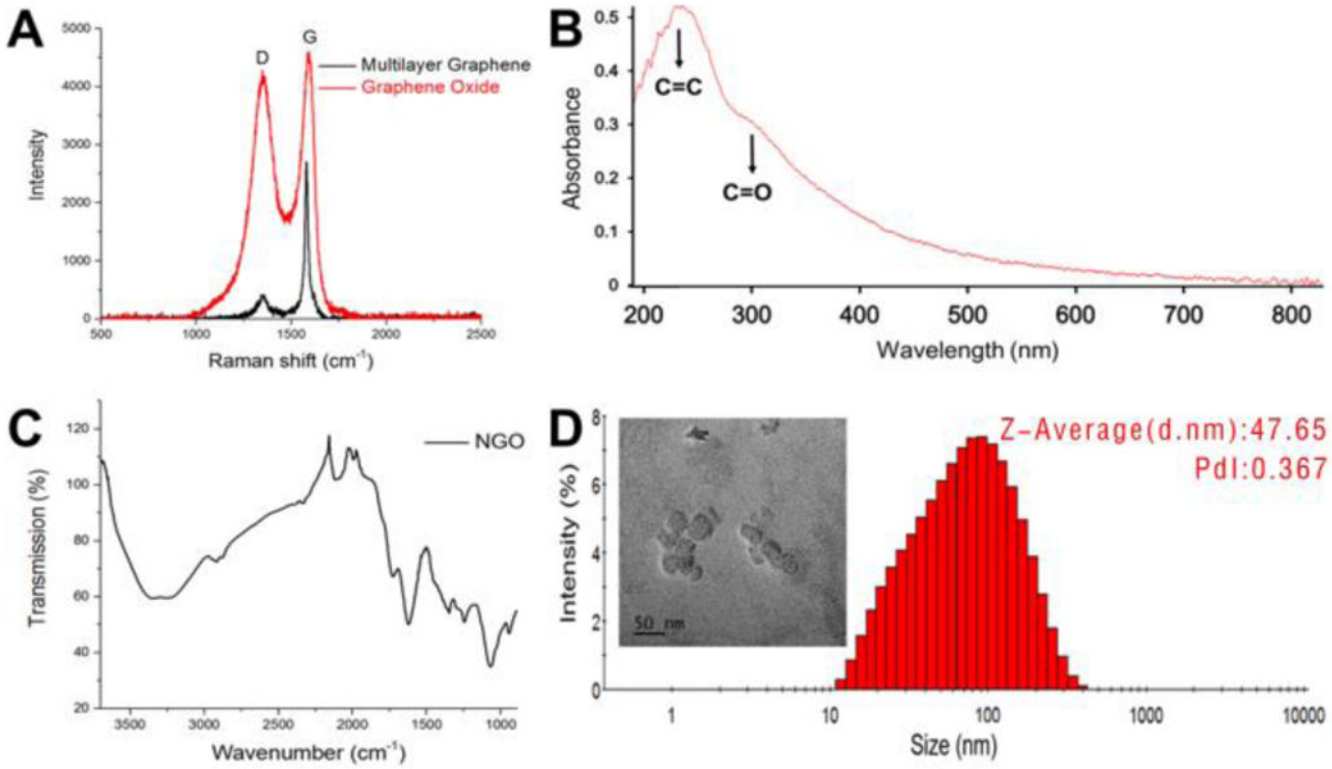

Fig. 2.

Characterizations of NGO. A) Raman spectra of NGO. The G peak of the graphene oxide becomes wider and shifted to 1585cm^{-1}, and the D peak at 1345cm^{-1} becomes stronger after oxidation. B) UV-vis spectra of NGO. The characteristic absorption peaks of C=O and C=C at 230 nm and 300 nm appeared. C) FT-IR spectra of NGO, which proved the presence of C=O at the edge of NGO at 1730 cm^{-1}. D) Hydrodynamic size distribution and TEM image (inset) of NGO. Scale bar is 100 nm.

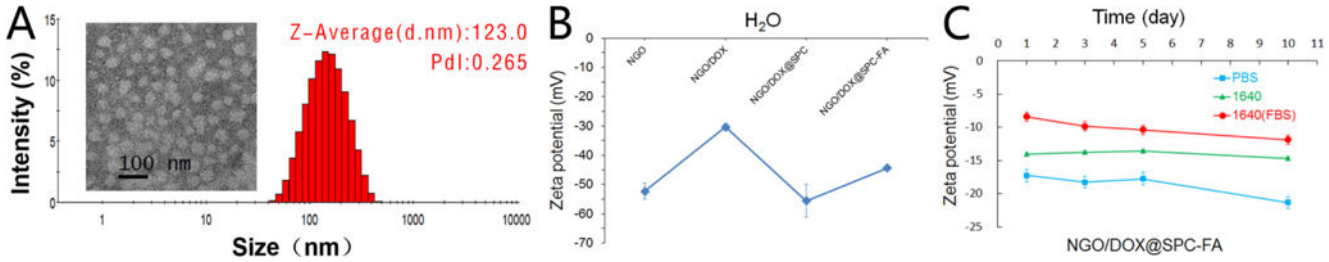

Fig. 3.

Characterization of NGO/DOX@SPC-FA. A) The result of TEM and DLS showed that the NGO/DOX@SPC-FA nanohybrids were round and about 100 nm wide. B) Zeta potential of NGO, NGO/DOX, NGO/DOX@SPC, NGO/DOX@SPC-FA in aqueous solution. The Zeta potential of NGO/DOX was higher than that of NGO because the positively charged amino groups on DOX were neutralized by NGO. The Zeta potential of NGO/DOX@SPC was lower than that of NGO/DOX because the amino group of DOX was shielded by the phospholipid bilayer, indirectly confirming the integration of phospholipid bilayer and NGO. The Zeta potential of NGO/DOX@SPC-FA was higher than that of NGO/DOX@SPC, which indicated that the amino group of FA was exposed and proved the modification of SPC membrane with FA. C) Zeta potential of NGO/DOX@SPC-FA nanohybrid in the various physiological solutions including PBS, 1640 medium and complete medium. The Zeta potential of NGO/DOX@SPC-FA was stable for 10 days in the different physiological solutions.

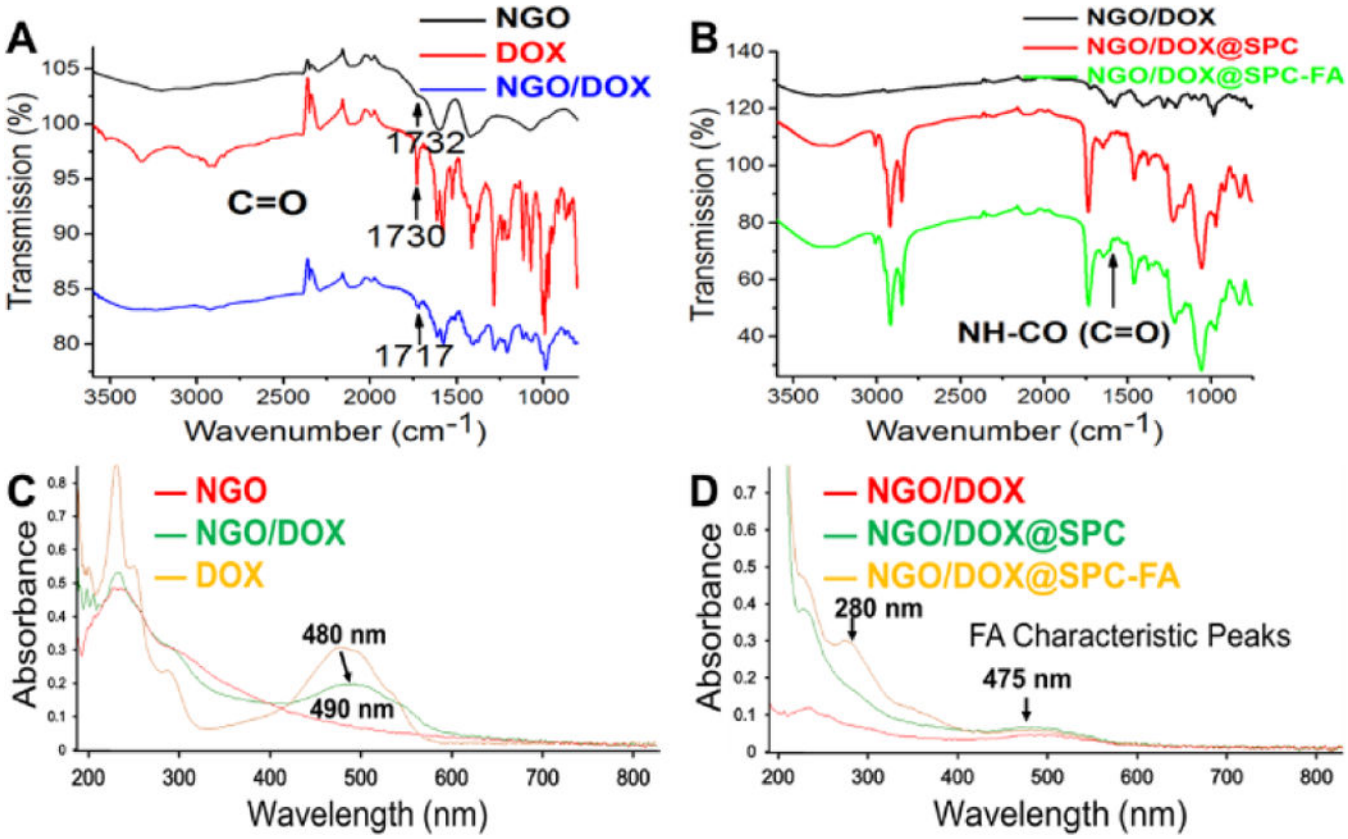

Fig. 4.

Spectroscopic characterization of nanohybrids. (A) FT-IR spectra of NGO, DOX, NGO/DOX. The C=O peak in NGO (at 1732 cm^{-1}) and DOX (1730 cm^{-1}) is slightly shifted to 1717 cm^{-1} after NGO/DOX complex were formed. (B) FT-IR spectra of NGO/DOX, NGO/DOX@SPC, NGO/DOX@SPC-FA. After NGO/DOX was coated with SPC to form NGO/DOX@SPC, the peaks at 2852 and 2922 cm^{-1}, attributable to νs(C-H) and νas(C-H) of $–CH_2$ in SPC, respectively, appear. The modification of NGO/DOX@SPC with FA to form NGO/DOX@SPC-FA was confirmed by the peaks at 1628 cm^{-1} corresponding to (-C=O-) of amide in the DSPE-PEG_{2000}-FA. (C) UV-vis spectra of NGO, DOX, and NGO/DOX in the aqueous solution. The peaks of DOX at 233 nm and 480 nm were shifted to 235 nm and 490 nm, respectively, after DOX was hybridized with NGO. (D) UV-vis spectra of NGO/DOX, NGO/DOX@SPC, NGO/DOX@SPC-FA in the aqueous solution. The characteristic peaks of FA at 280 nm and 475 nm confirm the coating of FA onto the NGO/DOX complex.

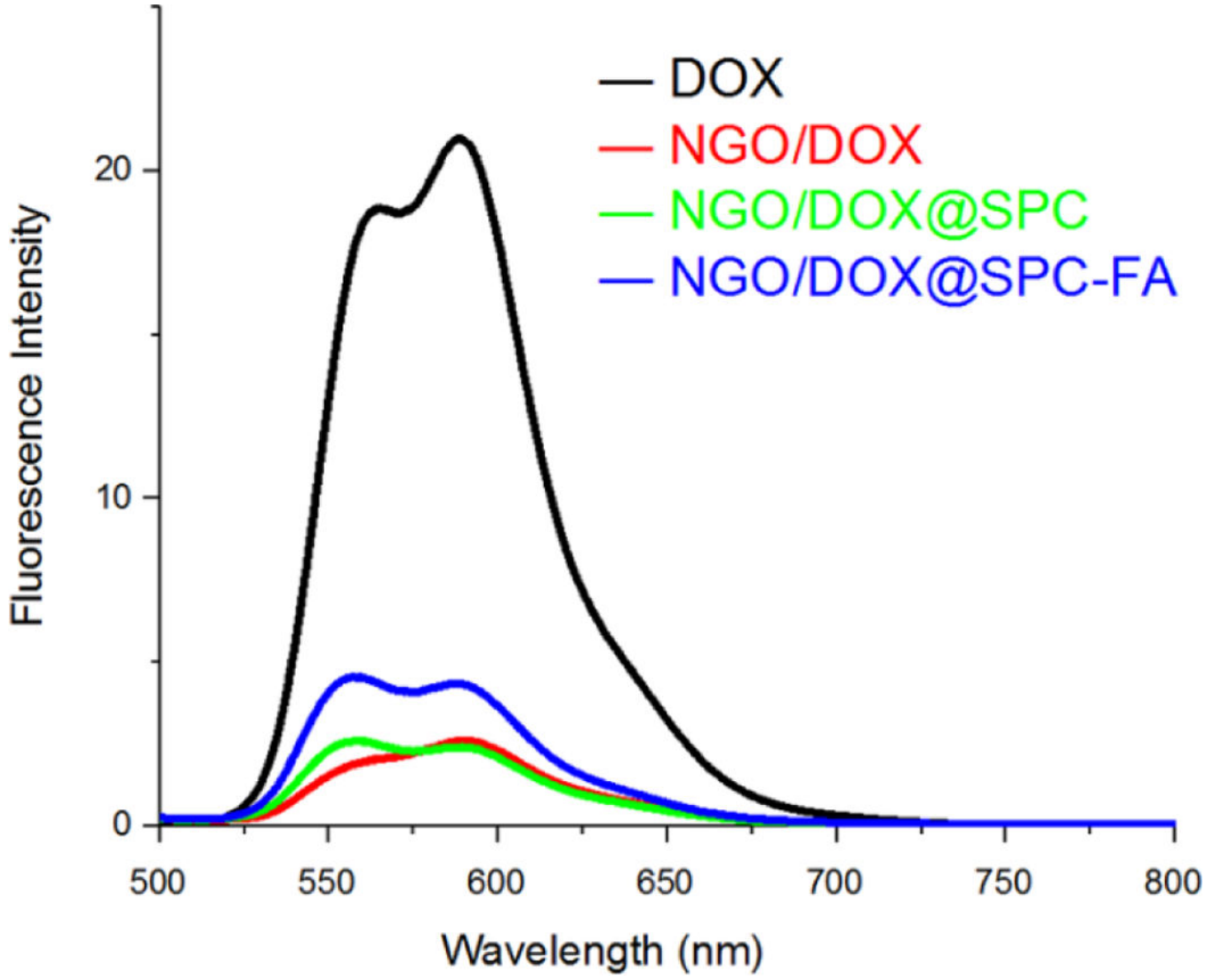

Fig. 5.

Fluorescence spectra of NGO, NGO/DOX, NGO/DOX@SPC, and NGO/DOX@SPC-FA in the aqueous solution. After the DOX was loaded on NGO, the fluorescence of DOX is quenched significantly. After the NGO/DOX was coated with SPC, the fluorescence quenching of DOX was still obvious, suggesting that the phospholipid bilayers did not detach DOX from NGO.

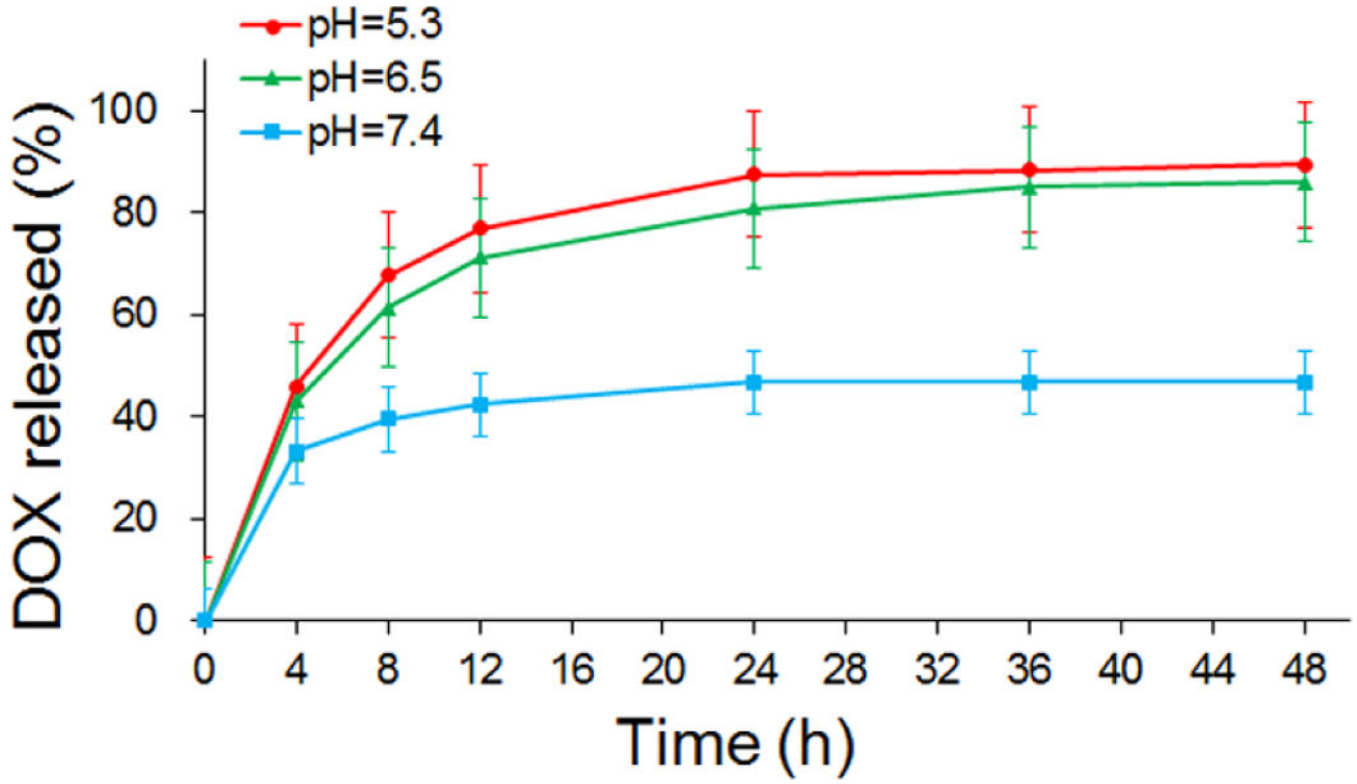

Fig. 6.

In vitro release of DOX from NGO/DOX@SPC-FA at different pH values. At pH 7.4, only 40% DOX was released from the nanohybrids within 48 h, but 90% and 85% of DOX was released from the nanohybrids at pH 5.3 and pH 6.5, respectively. This result demonstrated the pH responsive drug release of NGO/DOX@SPC-FA.

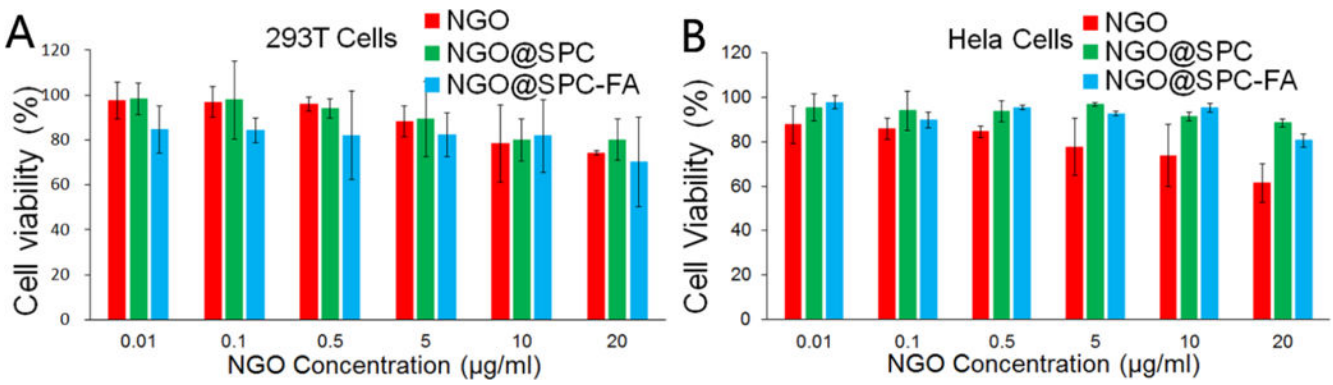

Fig. 7.

In vitro cytotoxicity of nanohybrids at different NGO concentrations. A) In vitro cytotoxicity of NGO, NGO@SPC and NGO@SPC-FA on 293T cells for 48 h. B) In vitro cytotoxicity of NGO, NGO@SPC and NGO@SPC-FA on Hela cells for 48h. No obvious toxicity was observed at all concentrations of these carriers. Data are presented as mean ±SD (n = 5).

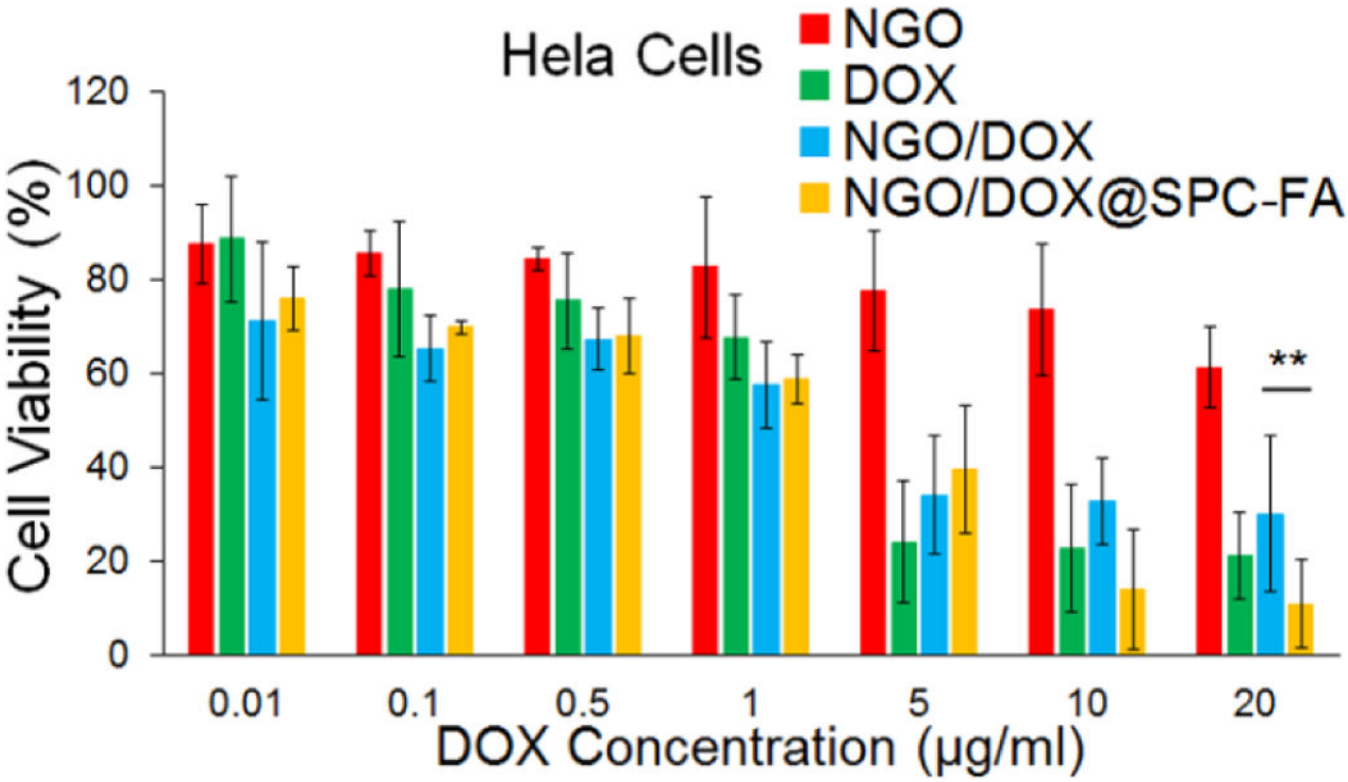

Fig. 8.

In vitro cytotoxicity of NGO, DOX, NGO/DOX@SPC and NGO/DOX@SPC-FA on Hela cells for 48 h at different DOX concentrations. The cytotoxicity of NGO was relatively negligible. The free DOX showed significant cytotoxicity above 5 μg/mL. After the DOX was loaded on NGO, the cytotoxicity of NGO/DOX was reduced. The NGO/DOX@SPC-FA showed higher cytotoxicity than free DOX and NGO/DOX at the concentrations over 10 μg/mL. **P ＜ 0.01. Data are presented as mean±SD (n = 5).

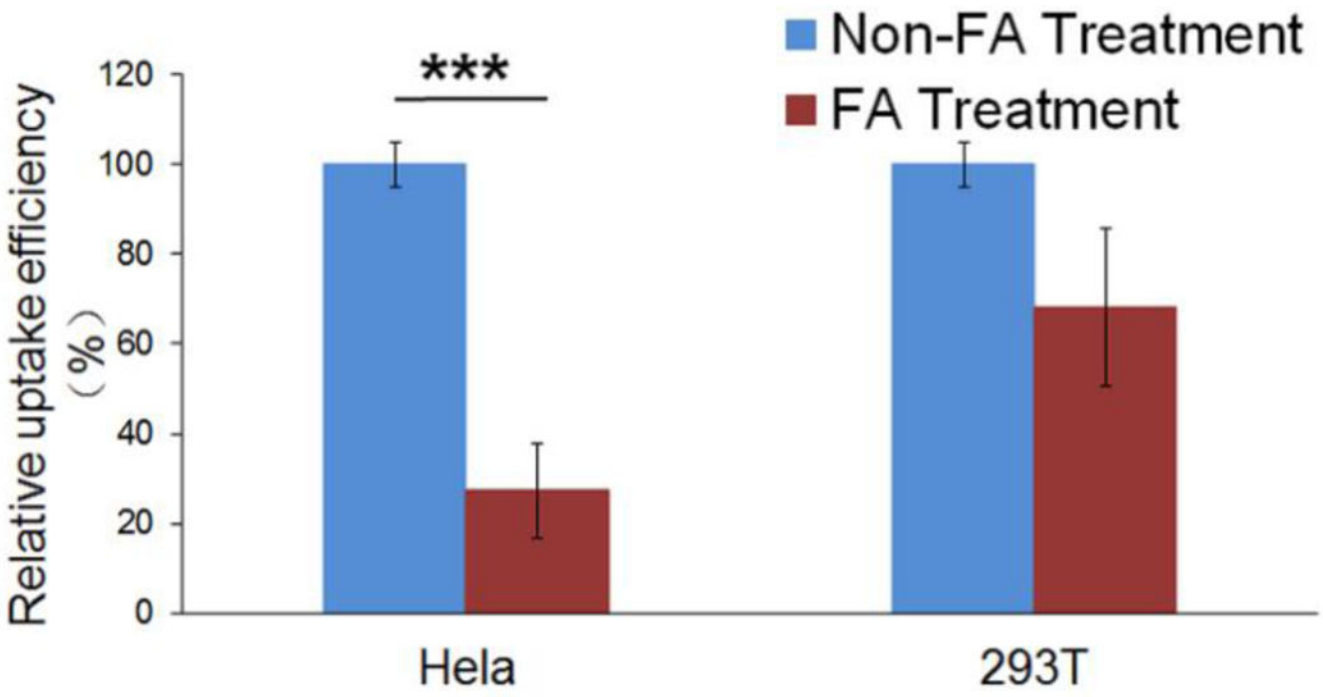

Fig. 9.

Relative uptake efficiency of NGO/DOX@SPC-FA in Hela and 293T cells with and without pretreatment with free FA. The difference in the cellular uptake of FA NPs in 293T cells between with and without pretreatment with free FA was not statistically different. However, the cellular uptake of NGO/DOX@SPC-FA nanohybrids decreased significantly in the Hela cells pretreated with free FA. ***P ＜ 0.001 versus their respective control. Data are presented as mean ±SD (n = 3).

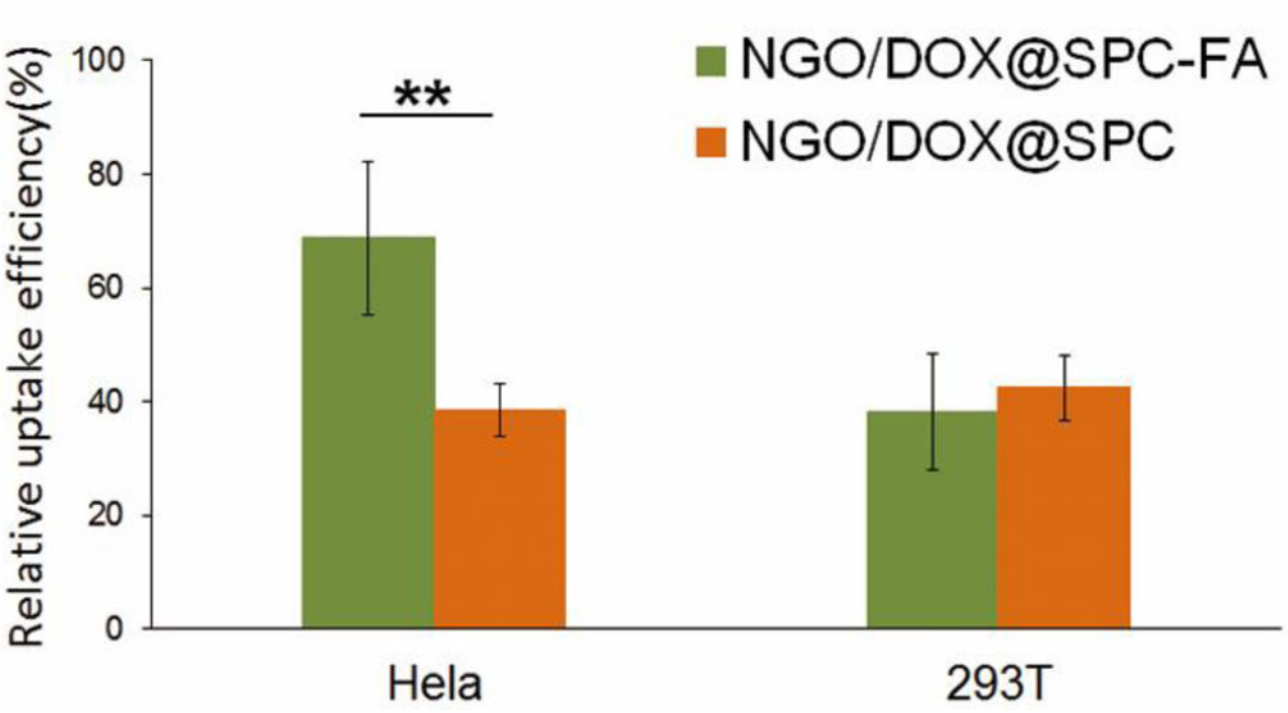

Fig. 10.

In vitro cellular uptake of NGO/DOX@SPC-FA and NGO/DOX@SPC in Hela and 293T cells for 24 h at 37°. The cellular uptake of NGO/DOX@SPC-FA was significantly higher than that of NGO/DOX@SPC in Hela cells, but the cellular uptake of NGO/DOX@SPC-FA and NGO/DOX@SPC was not statistically different in 293T cells. These results indicated the nanohybrids can realize tumor targeted delivery after being modified with FA. **P < 0.01 versus their respective control. Data are presented as mean ±SD (n = 3).

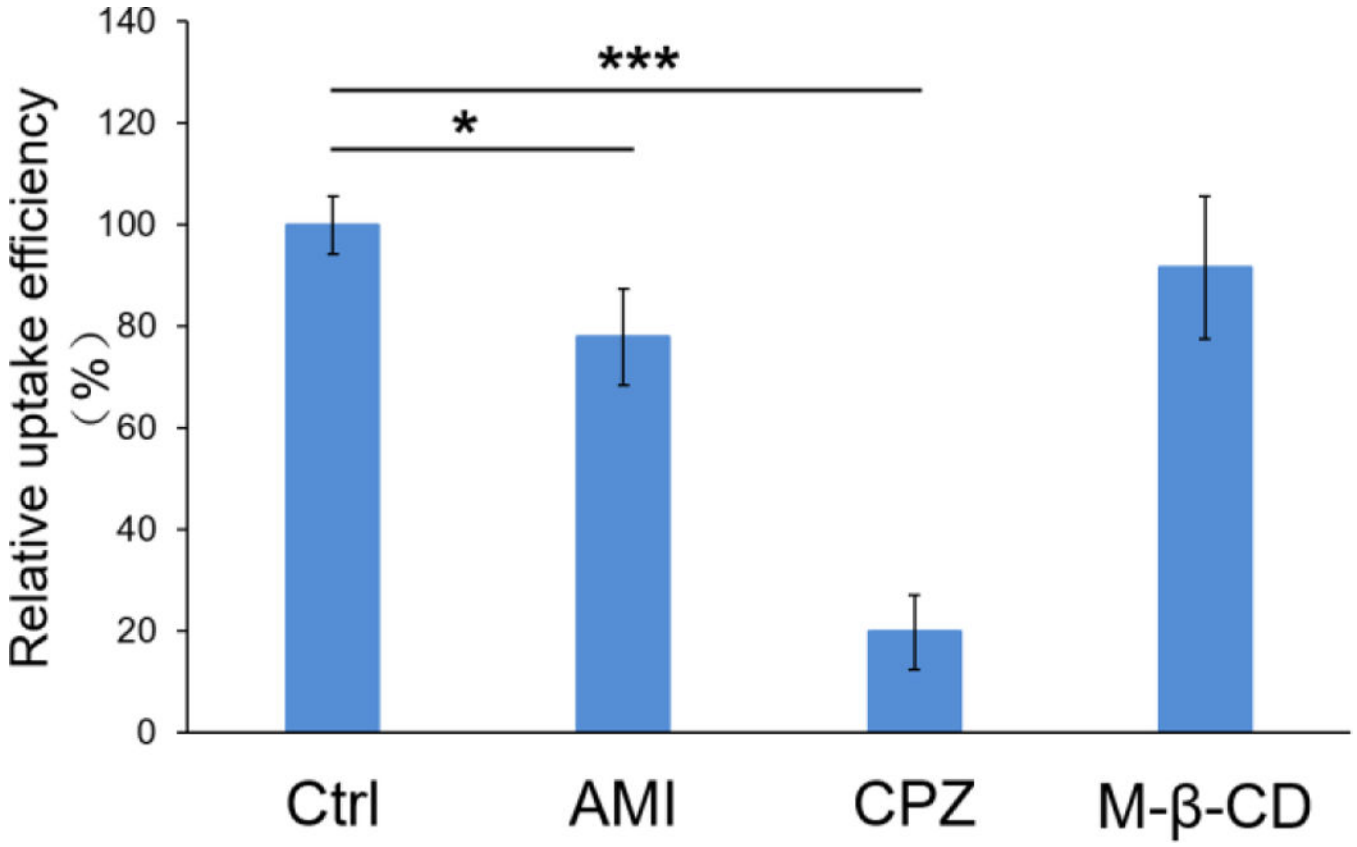

Fig. 11.

Relative uptake efficiency of NGO/DOX@SPC-FA in Hela cells pre-treated with various endocytosis inhibitors at 37°. CPZ treatment resulted in the decrease of 80% DOX uptake. AMI treatment led to a decrease of cellular uptake of DOX. M-β-CD treatment did not show any effect on nanohybrids uptake. *P < 0.05, ***P < 0.001 versus their respective control. Data are presented as mean ±SD (n = 3).

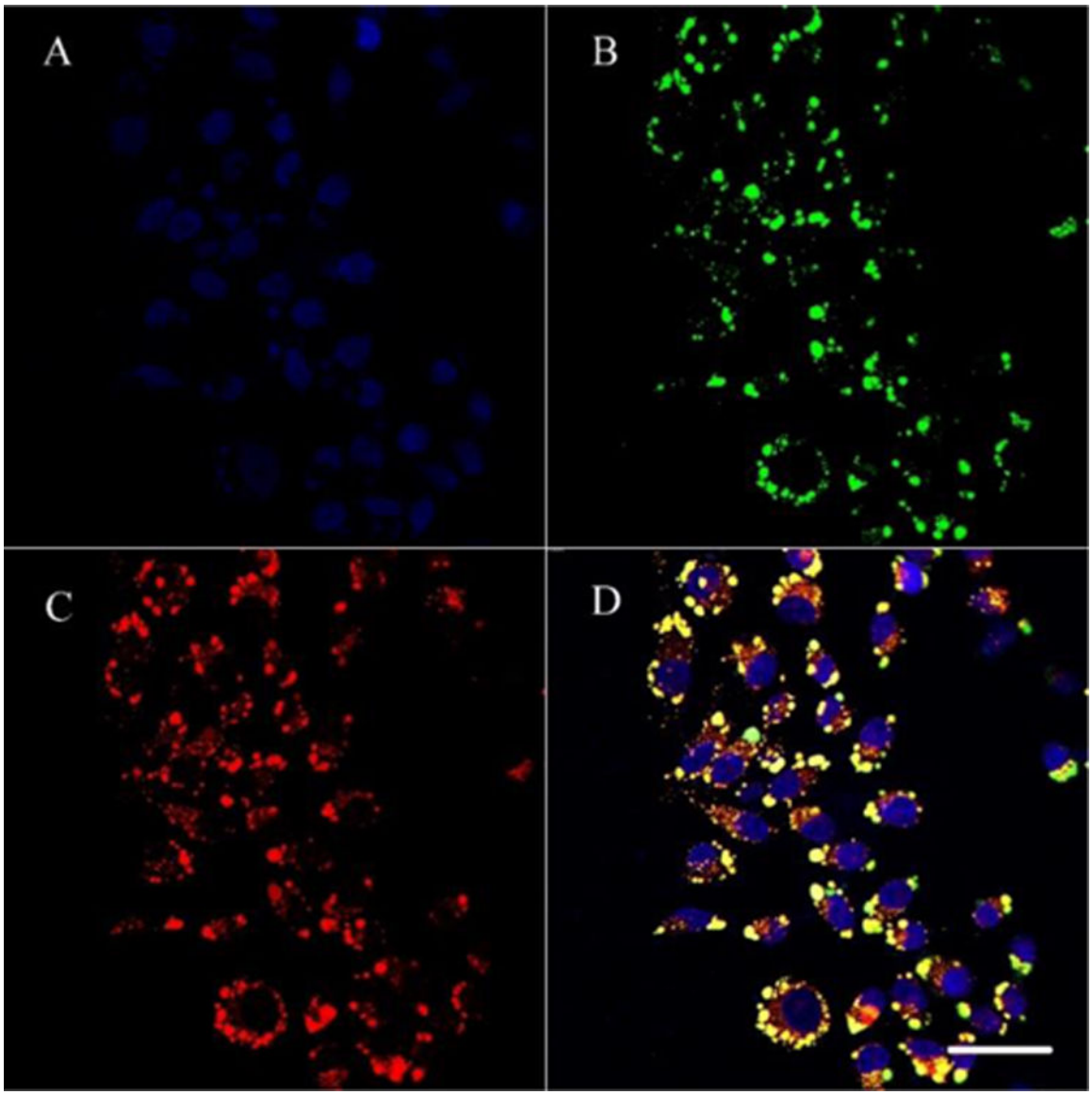

Fig. 12.

Intracellular delivery of NGO@SPC/Cou6-FA on Hela cells by CLSM. The lysosomes were stained by LysoTracker Red and the nuclei were stained by Hoechest 33342. A: blue-fluorescent Hoechest 33342; B: green-fluorescent Cou6; C: red-fluorescent lysosomes; D: overlay of A, B and C. The overlap yellow fluorescence confirmed that most of the endocytosed NGO@SPC/Cou6-FA were located in the lysosomes. Scale bars are 50 μm.

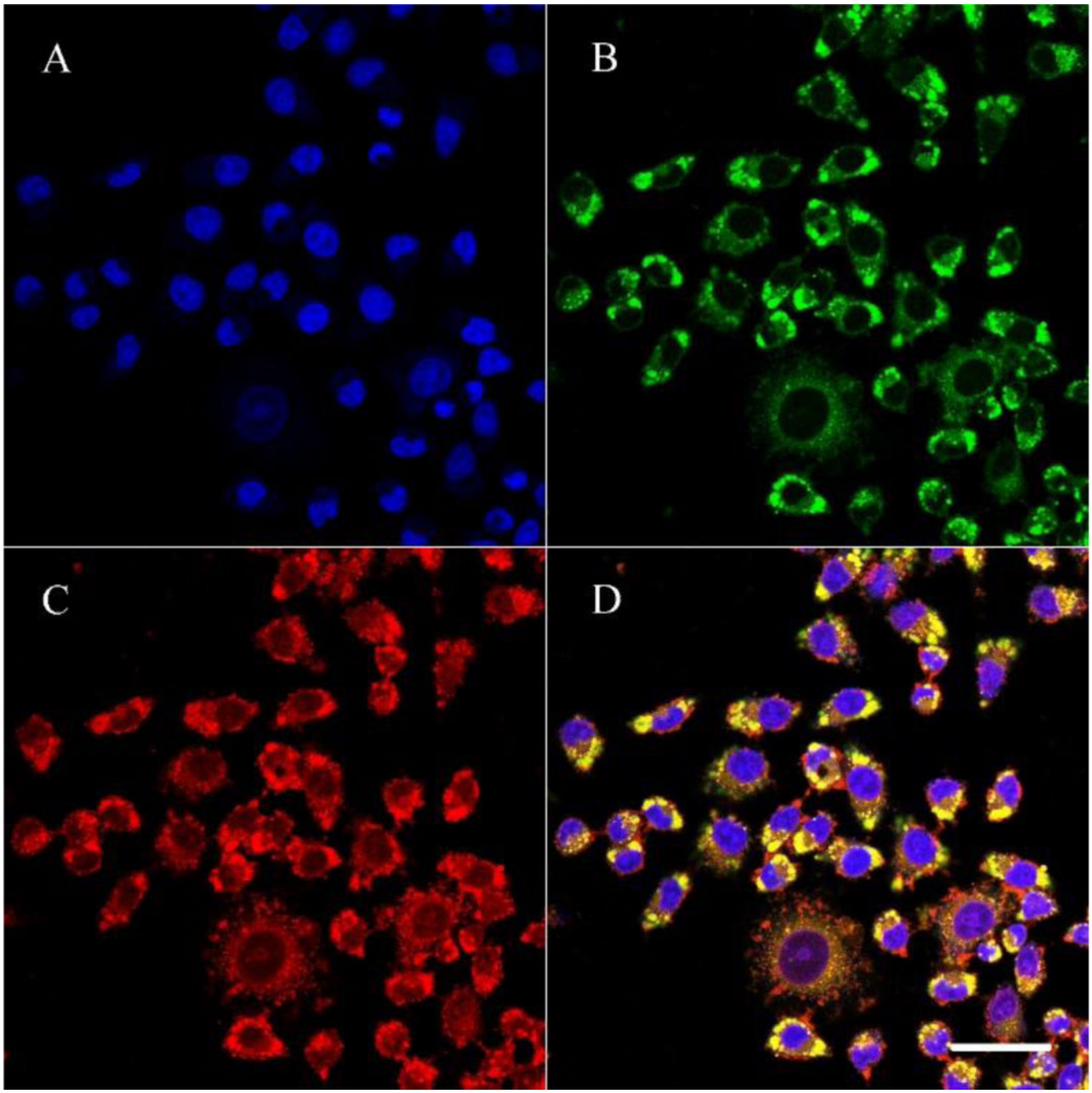

Fig. 13.

Intracellular distribution of NGO/DOX@SPC/Cou6-FA in Hela cells by confocal microscopy. The SPC lipids were stained by coumarine-6 and the nuclei were stained by Hoechest 33342. A: blue-fluorescent of Hoechest 33342; B: red-fluorescent of DOX; C: green-fluorescent of Cou6; D: overlay of A, B, and C. The overlap yellow fluorescence revealed that SPC and NGO/DOX of NGO/DOX@SPC-FA stayed together after taken up for 1 h by Hela cells. Scale bars are 50 μm.

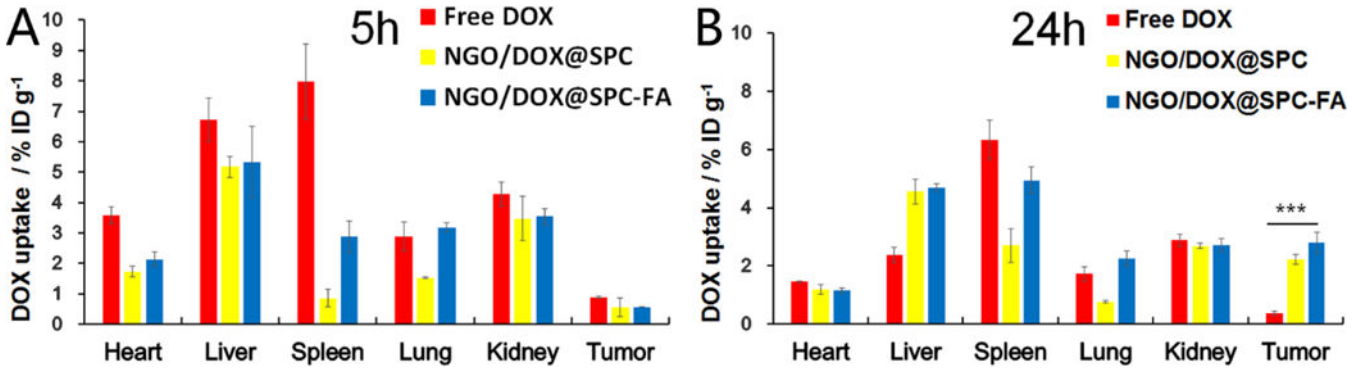

Fig. 14.

In vivo DOX biodistribution of free DOX, NGO/DOX@SPC, and NGO/DOX@SPC-FA after intravenous administration for the cervical tumour-bearing nude mice at 5 h (A) and 24 h (B). The tumour and normal organs were collected from the mice at 5 h and 24 h after administration, and then HPLC was used to analyze the accumulation of DOX in the tumour and normal organs. ***P ＜ 0.001 versus their respective control. Data are presented as mean ±SD (n = 3)

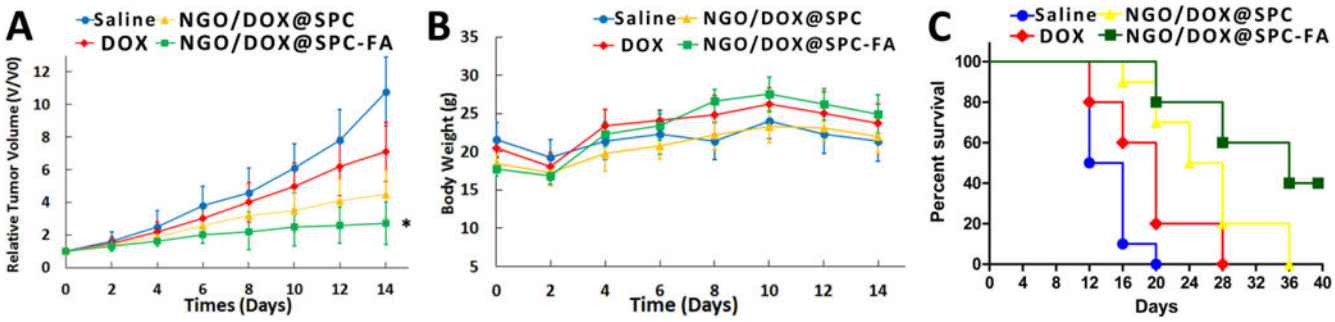

Figure 15.

In vivo antitumor activity of nanohybrids. (A) Time-dependent relative tumor volume in different treatment groups (saline, free DOX, NGO/DOX@SPC, NGO/DOX@SPC-FA). *P < 0.01 versus their respective control. Each point represents the mean ± SD (n = 5). (B) Time-dependent body-weight curves of mice in each experiment group. Data are presented as mean ±SD (n = 5). (C) Percent survival for different treatment groups.